Available online at www.sciencedirect.com
ScienceDirect
International Journal of Mass Spectrometry 267 (2007) 24–29
International Journal of Mass Spectrometry
www.elsevier.com/locate/ijms

Gaseous- versus solution-phase recognition of some aromatic amino esters by 2,8,14,20-tetrakis(*L*-valinamido)[4]resorcinarene

Bruno Botta *, Giuliano Delle Monache, Caterina Fraschetti, Laura Nevola, Deborah Subissati, Maurizio Speranza *

Dipartimento degli Studi di Chimica e Tecnologia delle Sostanze Biologicamente Attive, Università di Roma "La Sapienza", 00185 Roma, Italy

Received 2 August 2006; received in revised form 10 January 2007; accepted 20 February 2007
Available online 23 February 2007

In the memory of Dr. Sharon Lias, whose seminal contributions to mass spectrometry and ion thermochemistry have been a continuous source of inspiration

Abstract

The effects of the physical environment on the molecular recognition of some aromatic amino esters (A = 3-(3,4)dihydroxyphenyl)alanine methyl ester (**DOPA**$^{\mathbf{OMe}}$), 3-(3,4)dihydroxyphenyl)alanine ethyl ester (**DOPA**$^{\mathbf{OEt}}$) and tryptophan ethyl ester (**trp**$^{\mathbf{OEt}}$)) by the flattened-cone 2,8,14,20-tetrakis(*L*-valinamido)[4]resorcinarene (**1**$_{\mathbf{L}}$) have been investigated in both the gas-phase by ESI-MS spectrometry and in $CDCl_3$ solutions by ^1H and ^{13}C NMR spectroscopy. It is found that the non-covalent [**1**$_{\mathbf{L}}$·H·**DOPA**$^{\mathbf{OMe}}$]$^+$ and [**1**$_{\mathbf{L}}$·H·**DOPA**$^{\mathbf{OEt}}$]$^+$ complexes are stable in the gas-phase. The last one is stable in $CDCl_3$ solutions as well, while [**1**$_{\mathbf{L}}$·H·**trp**$^{\mathbf{OEt}}$]$^+$ is not. The formation of the stable [**1**$_{\mathbf{L}}$·H·**DOPA**$^{\mathbf{OEt}}$]$^+$ complex in $CDCl_3$ is not affected by the presence of traces of additives, like D_2O, DCl or ethyl acetate, or by absorption on silica. APT-^{13}C NMR analysis of [**1**$_{\mathbf{L}}$·H·**DOPA**$^{\mathbf{OEt}}$]$^+$ suggests that the amino ester is mainly located inside the resorcinarene cavity, in conformity with the most stable structure arising from MC/MD simulations.

Keywords: Host–guest system; Gas-phase kinetics; Enantioselectivity; Mass spectrometry; NMR spectroscopy

1. Introduction

Since intact non-covalent complexes have been observed for the first time by electrospray mass spectrometry (ESI-MS), the interest in the field has constantly been growing [1]. The stoichiometry, the stability constant, and the reactivity of non-covalent complexes can be determined so easily by ESI-MS that this methodology represents nowadays an essential tool for the identification and structural characterization of biomolecules, like proteins [2–8]. Indeed, much effort has been devoted to the ESI-MS study of the structures and binding strengths of unsolvated protein complexes and to the assessment of the intervening non-covalent interactions [9–11]. The validity of these pieces of information, referred to unsolvated systems, in reproducing the activity and selectivity of real biomolecules, normally operating in liquid media, is still open to question. By one side, gas-phase information reveals of utmost importance for modelling the selectivity and catalytic properties of proteic biopolymers, if one considers the extensive, if not complete desolvation of a guest molecule when entering the hydrophobic cavity of an enzyme. On the other side, no information is available on the origin of the charged complexes detected by ESI-MS, whether pre-formed in solution or generated in the ESI source by solvent evaporation of charged droplets. In other words, a mass detected non-covalent complex may be stable in the unsolvated state and representative of the same species stable in solution or, rather, it may be either unstable in solution or, if sufficiently stable, endowed with structural and reactivity properties completely different from those of the same unsolvated complex. These points have been addressed in the present comparative NMR and FT-ICR study.

2. Results and discussion

We took, as representative example, the complexes between the enantiomers of 3-(3,4-dihydroxyphenyl)-alanine esters (**DOPA**$^{\mathbf{OMe}}$ and **DOPA**$^{\mathbf{OEt}}$ in Fig. 1) and the amido[4]reso-

* Corresponding authors. Tel.: +39 06 49913497; fax: +39 06 49913602.
E-mail address: maurizio.speranza@uniroma1.it (M. Speranza).

1387-3806/$ – see front matter © 2007 Elsevier B.V. All rights reserved.
doi:10.1016/j.ijms.2007.02.015

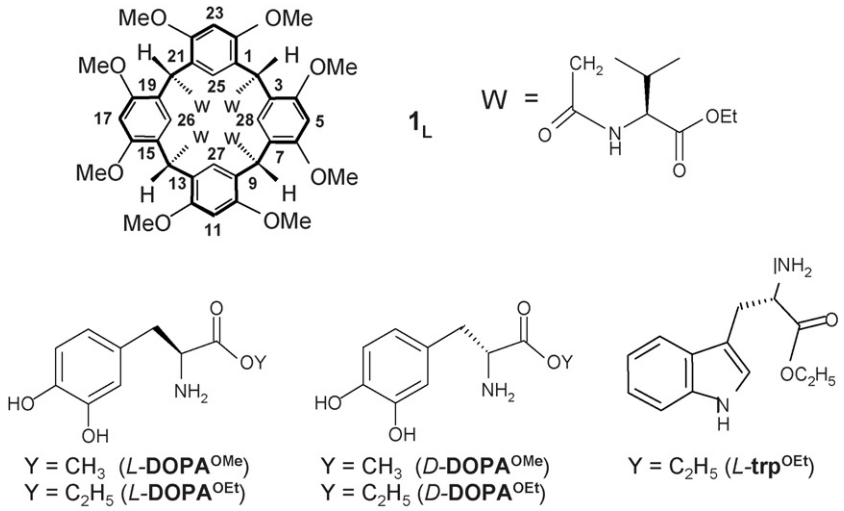

Fig. 1. Formula of flattened-cone 2,8,14,20-tetrakis(*L*-valinamido)[4] resorcinarene (**1**$_L$); formulae of the enantiomers of 3-(3,4-dihydroxyphenyl)-alanine methyl ester (**DOPA**^{OMe}); 3-(3,4-dihydroxyphenyl)-alanine ethyl ester (**DOPA**^{OEt}) and tryptophan ethyl ester (**trp**^{OEt}).

rcinarene **1**$_L$, a potential enzyme mimic. As shown in Fig. 1, macrocycle **1**$_L$ is endowed with a cavity-shaped dissymmetric architecture due to the presence of suitably located side chains (pendants W in Fig. 1) containing the chiral *L*-valine group.

This study comes into a more comprehensive FT-ICR investigation on the gas-phase enantioselectivity of the chiral microcycle **1**$_L$ towards a number of amino acid derivatives A [12–18]. The stability and reactivity of their proton-bonded diastereomeric complexes $[\mathbf{1}_L{\cdot}H{\cdot}A]^+$ was checked by measuring the rate of the loss of the A component by the action of the pure enantiomers of 2-aminobutane (B in Eq. (1)).

$$[\mathbf{1}_L{\cdot}H{\cdot}A]^+ + B \rightarrow A + [\mathbf{1}_L{\cdot}H{\cdot}B]^+ \quad (1)$$

On the grounds of the relevant kinetic results, we could appreciate *inter alia* the occurrence of at least two stable isomeric structures for $[\mathbf{1}_L{\cdot}H{\cdot}A]^+$ (A = 3-(3,4-dihydroxyphenyl)-alanine (**DOPA**), 3-(4-hydroxyphenyl)-alanine methyl ester (**tyr**^{OMe}) and tryptophan (**trp**) since the corresponding displacement reactions (1) invariably exhibit a bi-exponential kinetics, like shown in Fig. 2a. The time dependence of the more reactive isomer (*fast* channel; solid circles in Fig. 2a) can be inferred from the overall $[\mathbf{1}_L{\cdot}H{\cdot}A]^+$ decay (open circles in Fig. 2a) after subtracting the first-order decay of the less reactive isomer (*slow* channel; upper line of Fig. 2a). The two isomeric structures react with the amine B at rates differing by a factor ranging from ca. 48 to 90. The *Y*-intercepts of the first-order decay of the *fast* and the *slow* channel provide an estimate of their relative distribution. The same behaviour is presently observed for the diastereomeric $[\mathbf{1}_L{\cdot}H{\cdot}\mathbf{DOPA}^{OMe}]^+$ complexes, whereas the homologous $[\mathbf{1}_L{\cdot}H{\cdot}\mathbf{DOPA}^{OEt}]^+$ ones follow a mono-exponential kinetics (Fig. 2b).

Some important pieces of information on these stable isomeric structures were obtained by a computational approach [13,15]. Several low-energy structures for the diastereomeric $[\mathbf{1}_L{\cdot}H{\cdot}A]^+$ complexes have been recognized by molecular mechanics (MM) calculations (docking). Mixed-mode Monte Carlo and molecular dynamics (MC/MD) simulations, starting from the global minima of the docking-generated structures, resulted into only two collapsed structures, persisting for at least 20 ns, named *down* and *up* (Fig. 3) [19].

The more stable *down* regioisomer features the guest located in the three-dimensional region surrounded by the four chiral pendants of $[\mathbf{1}_L{\cdot}H]^+$ (*down* in Fig. 3) [19]. Conversely, in the

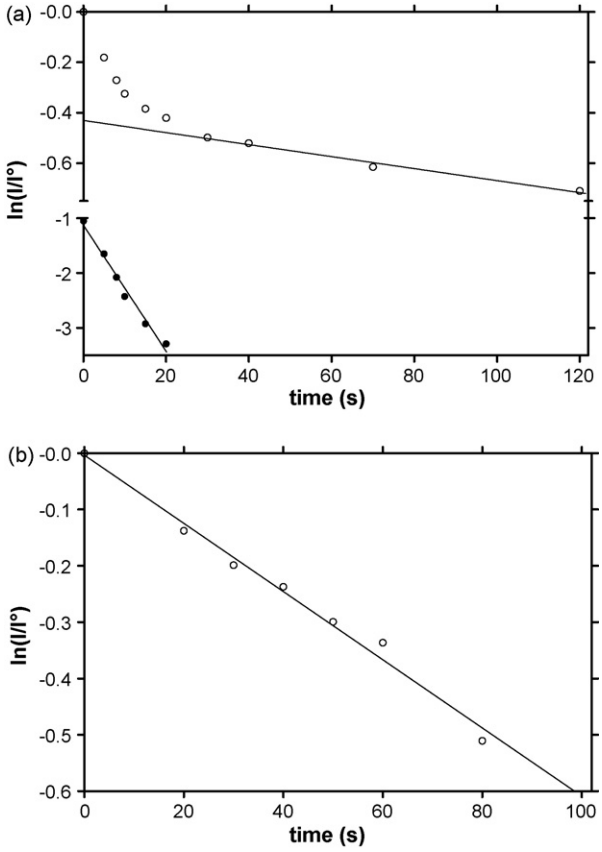

Fig. 2. (a) Kinetic plot for the gas-phase reaction between s-(+)-2-butylamine ($P_B = 1.4 \times 10^{-7}$ mbar) and $[\mathbf{1}_L{\cdot}H{\cdot}L\text{-}\mathbf{DOPA}^{OMe}]^+$. (b) Kinetic plot for the gas-phase reaction between s-(+)-2-butylamine ($P_B = 3.8 \times 10^{-7}$ mbar) and $[\mathbf{1}_L{\cdot}H{\cdot}L\text{-}\mathbf{DOPA}^{OEt}]^+$.

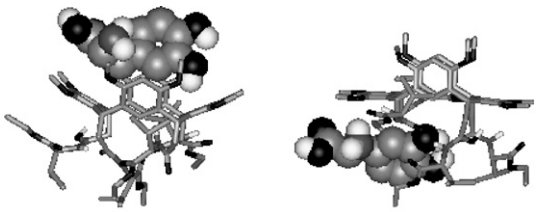

Fig. 3. Front view of the fully minimized structures of the *up* and *down* regioisomers of $[\mathbf{1_L}\cdot H\cdot \textit{D}\text{-}\mathbf{DOPA}]^+$. Similar structures have been obtained using $\mathbf{tyr^{OMe}}$ and **trp**, as guests (refs. [15,16]).

Table 1
Percent distribution of isomeric $[\mathbf{1_L}\cdot H\cdot A]^+$ structures

Guest (A)	$[\mathbf{1_L}\cdot H\cdot A]^+_{fast}$	$[\mathbf{1_L}\cdot H\cdot A]^+_{slow}$	Source
D-$\mathbf{tyr^{OMe}}$	20 ± 3	80 ± 3	Ref. [16]
L-$\mathbf{tyr^{OMe}}$	23 ± 2	77 ± 2	Ref. [16]
D-**trp**	32 ± 5	68 ± 5	Refs. [15,16]
L-**trp**	35 ± 3	65 ± 3	Refs. [15,16]
D-**DOPA**	20 ± 4	80 ± 4	Refs. [13,14]
L-**DOPA**	19 ± 3	81 ± 3	Refs. [13,14]
D-$\mathbf{DOPA^{OMe}}$	11 ± 6	89 ± 6	This work
L-$\mathbf{DOPA^{OMe}}$	26 ± 9	74 ± 9	This work
D-$\mathbf{DOPA^{OEt}}$	–	100	This work
L-$\mathbf{DOPA^{OEt}}$	–	100	This work

less stable *up* regioisomer, the guest is placed in the achiral upper-rim cavity of $[\mathbf{1_L}\cdot H]^+$ (*up* in Fig. 3). The most stable *down* regioisomer is identified as responsible of the *slow* component of the bi-exponential decay curve of Fig. 2a, whereas the *fast* component of the curve is obviously attributed to the less stable *up* regioisomer.

Table 1 reports the relative distribution of the two $[\mathbf{1_L}\cdot H\cdot A]^+$ regioisomers estimated from kinetic analysis of the corresponding kinetic curves. Table 2 gives the rate constants k for all the displacement reactions (1), together with the relevant enantioselectivity factors ρ and ξ. The ρ term measures the effect of the amino acid configuration on the exchange reaction, while the ξ parameter weights the effect of the amine B configuration on the exchange reaction. A $\rho > 1$ value indicates that the amine B displaces the D-enantiomer of A (A_D) faster that the L-enantiomer (A_L) from the relevant diastereomeric $[\mathbf{1_L}\cdot H\cdot A_D]^+$ and $[\mathbf{1_L}\cdot H\cdot A_L]^+$ complexes. The opposite is true when $\rho < 1$. A $\rho = 1$ value corresponds to equal displacement rates. Analogously, a $\xi > 1$ value indicates that the displacement of the A guest from a given $[\mathbf{1_L}\cdot H\cdot A]^+$ diastereomer is faster with the R-amine (B_R) than with the S-one (B_S). Again, the opposite is true when $\xi < 1$. A $\xi = 1$ value corresponds to equal displacement rates. On the grounds of the ρ and ξ factors, shown in Table 2, it is evident that the efficiency of the gas-phase exchange reaction (1) is appreciably dependent not only on the configuration of both A and B, but also on the specific structure (*down* or *up*) of the starting $[\mathbf{1_L}\cdot H\cdot A]^+$ complex.

Once having ascertained the occurrence and the long lifetime of the selected $[\mathbf{1_L}\cdot H\cdot A]^+$ complexes in the gas-phase (at least of the order of minutes in the FT-ICR cell), the following step was to verify whether the same complexes are actually formed in solution. For this purpose, two solutions of free *L*-$\mathbf{DOPA^{OEt}}$ in $CDCl_3$ (0.8 mL, 20 μmol/mL) were prepared

Table 2
Exchange rate constants ($k \times 10^{-12}$ cm^3 molecule^{-1} s^{-1})

Guest (A)		(R)-(−)-$C_4H_9NH_2$			(S)-(+)-$C_4H_9NH_2$			ξ
		k	Eff. (%)[a]	ρ	k	Eff. (%)[a]	ρ	
D-$\mathbf{tyr^{OMe}}$	Fast	163 ± 19	14.6	0.62 ± 0.17	130 ± 4	11.7	0.72 ± 0.10	1.25 ± 0.19
L-$\mathbf{tyr^{OMe}}$	Fast	261 ± 30	23.4		180 ± 9	16.2		1.45 ± 0.25
D-$\mathbf{tyr^{OMe}}$	Slow	12 ± 1	1.04	0.63 ± 0.06	8 ± 1	0.73	0.51 ± 0.07	1.43 ± 0.15
L-$\mathbf{tyr^{OMe}}$	Slow	18 ± 1	1.64		16 ± 1	1.41		1.17 ± 0.11
D-**trp**	Fast	182 ± 4	15.7	1.60 ± 0.11	192 ± 4	16.6	0.82 ± 0.10	0.95 ± 0.04
L-**trp**	Fast	114 ± 4	9.8		233 ± 20	20.1		0.49 ± 0.06
D-**trp**	Slow	15 ± 1	1.30	1.07 ± 0.13	23 ± 1	1.99	0.62 ± 0.18	0.65 ± 0.04
L-**trp**	Slow	14 ± 1	1.21		37 ± 7	3.20		0.37 ± 0.09
D-**DOPA**	Fast	228 ± 8	20.4	0.76 ± 0.04	126 ± 5	11.3	0.69 ± 0.11	1.81 ± 0.12
L-**DOPA**	Fast	300 ± 9	26.9		182 ± 20	16.3		1.65 ± 0.24
D-**DOPA**	Slow	7.3 ± 0.8	0.65	0.73 ± 0.13	6.4 ± 0.8	0.57	0.81 ± 0.19	1.14 ± 0.28
L-**DOPA**	Slow	10.0 ± 0.8	0.90		7.9 ± 0.9	0.71		1.27 ± 0.25
D-$\mathbf{DOPA^{OMe}}$	Fast	169 ± 13	14.5	2.73 ± 0.45	45 ± 5	3.8	0.85 ± 0.16	3.75 ± 0.63
L-$\mathbf{DOPA^{OMe}}$	Fast	62 ± 7	5.3		53 ± 3	4.5		1.17 ± 0.21
D-$\mathbf{DOPA^{OMe}}$	Slow	1.88 ± 0.03	0.16	1.92 ± 0.12	0.93 ± 0.07	0.08	0.84 ± 0.15	2.02 ± 0.17
L-$\mathbf{DOPA^{OMe}}$	Slow	0.98 ± 0.04	0.08		1.10 ± 0.09	0.09		0.89 ± 0.12
D-$\mathbf{DOPA^{OEt}}$		0.62 ± 0.03	0.05	0.59 ± 0.07	0.57 ± 0.02	0.05	0.55 ± 0.04	1.09 ± 0.09
L-$\mathbf{DOPA^{OEt}}$		1.04 ± 0.05	0.09		1.03 ± 0.04	0.09		1.01 ± 0.09

[a] The reaction efficiency (eff) is calculated as the percent ratio between the measured rate constants and the corresponding collision constant k_C, calculated using the trajectory calculation method [25].

by adding $NaHCO_3/D_2O$ to the corresponding hydrochloride. Aliquots (0.2 mL) of one solution were added to an equimolar solution of $\mathbf{1_L}$ in $CDCl_3$ up to reaching the stoichiometric 1:1 equivalence. After each addition, the mixture (henceforth denoted as $G \rightarrow H$) was submitted to ^1H and APT-^{13}C NMR analysis. A second set of NMR spectra has been recorded for the second solution by inverting the addition sequence (henceforth denoted as $H \rightarrow G$). In both cases, it was not possible to elaborate a titration curve.

As regards to the ^1H NMR signals pertaining the amino estereal guest, they were affected by the presence of residual D_2O. In particular, the OH and the NH_2 groups of *L*-**DOPA^{OEt}**, as well as its H-2 aromatic proton undergo effective H/D exchange. The consequence was that the signals for to the H-5 and H-6 aromatic protons appeared as doublets so broad to prevent any conceivable discrimination between complexed and free amino ester. Concerning the APT-^{13}C NMR signals of the guest, the carbon resonances of *L*-**DOPA^{OEt}** in $H \rightarrow G$ mixtures were flanked by smaller peaks, even though not assignable in values. The situation was even worse for the APT-^{13}C NMR signals of *L*-**DOPA^{OEt}** in the guest-poor $G \rightarrow H$ mixtures.

The ^1H NMR signals pertaining the amido[4]resorcinarene $\mathbf{1_L}$ host were also affected by the presence of residual D_2O. In particular, effective H/D exchange was observed between D_2O and the NH group of the *L*-valine pendants (W in Fig. 1), as well as the family of the H_e protons at C-5/11/17/23 of $\mathbf{1_L}$. Small satellite signals were observed in the ^1H NMR spectra of $G \rightarrow H$ solutions, but, as mentioned above, they were not utilizable for a titration curve. The corresponding APT-^{13}C NMR spectra are much more informative, since two separate signals for almost all carbons of the macrocyclic host could be discerned and were attributed to free (major) and complexed $\mathbf{1_L}$ (minor). A question now arises as to the nature of the complexed $\mathbf{1_L}$, whether it contains the *L*-**DOPA^{OEt}** or else. To resolve this doubt, the equivalent fractions of the final $H \rightarrow G$ and $G \rightarrow H$ solutions were pooled and the solvent evaporated under vacuum. TLC analysis (silica gel; $CHCl_3$-EtOAc-MeOH, 90:7:3, two runs) of an aliquot of the solid residue revealed (UV light; H_2SO_4:MeOH = 1:10 spray) the presence of two components, which were separated by column chromatography (CC; silica gel, $CHCl_3$:EtOAc = 80:20). The major, less polar component, recognized as the free $\mathbf{1_L}$ by ^1H NMR analysis and by TLC comparison with an authentic sample, provided a ESI-MS spectra characterized by the *m/z* 1341.6, $[\mathbf{1_L}\cdot H]^+$) and *m/z* 1363.7, $[\mathbf{1_L}\cdot Na]^+$ fragments. The minor, more polar component, recognized as a complexed $\mathbf{1_L}$ by ^1H NMR analysis, gave an ESI-MS spectrum characterized by the natural isotopic distribution of two ionic species starting at *m/z* 1567.8 ($[\mathbf{1_L}\cdot H\cdot$*L*-**DOPA^{OEt}**$]^+$) and at 1589.8 ($[\mathbf{1_L}\cdot Na\cdot$*L*-**DOPA^{OEt}**$]^+$). No signs of heavier fragments were detected, thus supporting the hypothesis of a stable complex between $\mathbf{1_L}$ and *L*-**DOPA^{OEt}** [20]. Notably, 20-eV collision induced dissociation (CID) of the isolated *m/z* 1567.8 ion ($[\mathbf{1_L}\cdot H\cdot$*L*-**DOPA^{OEt}**$]^+$) yields exclusively the corresponding $[\mathbf{1}\cdot H]^+$ fragment (*m/z* 1341.6), as expected from the non-covalent $[\mathbf{1_L}\cdot H\cdot$*L*-**DOPA^{OEt}**$]^+$complex. Incidentally, the observation of the $[\mathbf{1_L}\cdot Na]^+$ and $[\mathbf{1_L}\cdot Na\cdot$*L*-**DOPA^{OEt}**$]^+$ ions, together with their $[\mathbf{1_L}\cdot H]^+$ and $[\mathbf{1_L}\cdot H\cdot$*L*-**DOPA^{OEt}**$]^+$ analogues, is due to the exceedingly large affinity of $\mathbf{1_L}$ for the Na^+ cations which are ubiquitous in polar solutions kept in glassy containers.

Table 3
APT-^{13}C NMR spectrum of a mixture (ca. 1:1) of $\mathbf{1_L}$ and *L*-**DOPA^{OEt}**

Carbon	δC (major)	δC (minor)	Δδ
C═O	172.92	172.75	+0.17
C═O	172.65	172.12	+0.43
C─O	156.07	156.04	+0.03
CH_i	127.29	127.29	0
C─C	123.57	124.03	−0.46
CD_e	95.87	96.02	−0.15
OCH_2 (Et)	60.79	61.09	−0.30
CHN	57.39	57.30	+0.09
OMe	55.99	55.91	+0.09
CH_2	40.73	41.28	−0.55
CH (iPr)	33.76	33.24	+0.52
CH	30.96	31.22	−0.28
Me (iPr)	18.75	18.62	+0.13
Me (iPr)	18.04	18.13	−0.09
Me (Et)	14.13	14.16	−0.03

Having assessed the identity of the guest trapped by $\mathbf{1_L}$, a further question arises as to whether the components of the corresponding complex are both neutral or one of them is protonated. Indeed, the equilibrium constant between neutral and protonated *L*-**DOPA^{OEt}**, which is obviously extremely small in apolar aprotic solvents like $CDCl_3$, may significantly increase in the proximity or even inside the polar protic cavity of macrocycle $\mathbf{1_L}$. A similar effect has been recently described concerning the stabilization of zwitterionic forms of amino acids in the gas-phase depending upon their position relative to the hydrophilic lower rim of the cyclodextrin cavity [21,22]. To answer the above question, the remaining aliquot of the solid residue obtained by evaporating the combined $H \rightarrow G$ and $G \rightarrow H$ solutions was dissolved in fresh $CDCl_3$ (0.8 mL) and the solution washed with D_2O:DCl = 10:1 (0.2 mL). Notably, the treatment with acid not only removed the signals of free *L*-**DOPA^{OEt}** from the NMR spectra, but also displayed better resolved couples of signals in the APT-^{13}C NMR spectrum (Table 3). This observation agrees with the hypothesis that protonated *L*-**DOPA^{OEt}** is trapped in the hydrophilic cavity of $\mathbf{1_L}$. The appearance of two separated signals for almost all the carbons of the host supports the presence of the proton-bound $[\mathbf{1_L}\cdot H\cdot$*L*-**DOPA^{OEt}**$]^+$ complex together with free $\mathbf{1_L}$ [20]. If we assume a positive (upfield) Δδ shift as due to the proximity effect of the guest, the results of Table 3 suggest that *L*-**DOPA^{OEt}** is located in the lower rim of the macrocycle inside its cavity with a structure closely resembling the *down* structure predicted by calculations. The resonances of the complexed *L*-**DOPA^{OEt}** could not be detected in view of the unfavourable stoichiometric ratio 4:1 between the carbon units of the pendants of $\mathbf{1_L}$ and those of *L*-**DOPA^{OEt}**.

The entire procedure has been repeated using tryptophan ethyl ester *L*-**trp^{OEt}** as a guest, instead of *L*-**DOPA^{OEt}**. In this case, the NMR analysis did not show any sign of complexation of *L*-**trp^{OEt}** by $\mathbf{1_L}$ under the same experimental conditions. The conclusive CC of $\mathbf{1_L}$/*L*-**trp^{OEt}** mixtures afforded only free $\mathbf{1_L}$ and *L*-**trp^{OEt}**. However, the experiment could exclude that the

doubling of carbon resonances, observed for the **1**$_L$/*L*-**DOPA**^{OEt} mixtures, were caused by the relatively drastic conditions used.

In conclusion, the present study indicates that: (1) the proton-bound [**1**$_L$·H·*L*-**DOPA**^{OEt}]$^+$ complex is stable not only in the gas-phase, but also in $CDCl_3$ solution. By contrast, no complexes between **1**$_L$ and *L*-**trp**^{OEt} are observable in $CDCl_3$ solution. A plausible reason for such a difference could be found in the lower polarity of *L*-**trp**^{OEt}, as compared to that of the *L*-**DOPA**^{OEt} guest; (2) the formation of the stable [**1**$_L$·H·*L*-**DOPA**^{OEt}]$^+$ complex in $CDCl_3$ is not affected by the presence of traces of D_2O; (3) the [**1**$_L$·H·*L*-**DOPA**^{OEt}]$^+$ complex endures also contacts with DCl/D_2O (washing procedure), as well as $CHCl_3$/EtOAc on silica gel (CC); (4) the APT-^{13}C NMR analysis of [**1**$_L$·H·*L*-**DOPA**^{OEt}]$^+$ suggests that the guest is mainly located inside the host cavity, in conformity with the most stable structure arisen from MC/MD simulations.

3. Material and methods

3.1. Materials

BF_3·Et_2O-induced tetramerisation of (*L*)-(*E*)-*N*-1-(carboxyethyl)-2-methylpropyl)-2,4-dimethoxycinnamate has been used in previous studies to synthesize the amido[4] resorcinarene **1**$_L$ in the cone geometry, together with three other stereoisomers (1,2-alternate, chair-1 and chair-2) [23]. The synthetic procedure has been greatly improved in the present study to obtain **1**$_L$ in a much better yield and purity**.** Resorc[4]arene tetraester (W = CH_2COOEt in Fig. 1), in the cone geometry [24], was hydrolyzed (2N NaOH; EtOH-H_2O, 2:1, reflux, 4 h) to the corresponding tetraacid (W = CH_2COOH in Fig. 1) and, then, quantitatively transformed into its acid chloride derivative (W = CH_2COCl in Fig. 1), using thionyl chloride in THF (reflux, 4 h). Diisopropylethylamine (DIPEA) was then added to the THF solution of the acid chloride derivative, under N_2, and the resulting mixture stirred at room temperature for 20 min. A *L*-Val-OMe·HCl/THF solution was then added dropwise to yield eventually the amido[4]resorcinarene **1**$_L$ (95% yield) which was purified by preparative HPLC and characterized by conventional NMR, FT-IR and ESI-MS analyses. Notably, the coincident rotatory powers of **1**$_L$ from two different preparations exclude any conceivable racemization of the *L*-Val-OMe groups during the last step of both reactions.

A simple and safe procedure was used to prepare the pure enantiomers of amino esters *L*-**DOPA**^{OMe}, *L*-**DOPA**^{OEt} and *L*-**trp**^{OEt}. Acetyl chloride (5 mL) was added dropwise to cooled dry ROH (either MeOH or EtOH, 50 mL; $T = 0\,^{\circ}C$), in which the corresponding amino acid (1.7 mmol) has been dissolved. The mixture was ed under reflux for about 2 h, and then evaporated to dryness. Aldrich Co. provided the pure R-(−) and S-(+) enantiomers of 2-butylamine, which were degassed in the vacuum manifold with several freeze–thaw cycles.

Melting points were recorded on a Büchi B-545 microscope, and are uncorrected. FT-IR spectra were recorded as KBr pellets on a Jasco FT/IR 430 spectrometer (Jasco Europe). Optical rotation values were determined on a Jasco P-1030 polarimeter at 20 °C (concentrations expressed in g/100 mL; solvent: methanol).

3.2. Mass spectrometric experiments

The FT-ICR experiments were performed at room temperature in an APEX 47 e FT-ICR mass spectrometer equipped with an ESI source (Bruker Spectrospin) and a resonance cell ("infinity cell") situated between the poles of a superconducting magnet (4.7 T) [12–16]. Stock solutions of **1**$_L$ (1×10^{-5} M) in H_2O/CH_3OH = 1:3, containing a five-fold excess of the appropriate amino ester A, were electrosprayed through a heated capillary (130 °C) into the external source of the FT-ICR mass spectrometer. The resulting ions were transferred into the resonance cell by a system of potentials and lenses and quenched by collisions with methane pulsed into the cell through a magnetic valve. Abundant signals, corresponding to the natural isotopic distribution of the proton-bound complex [**1**$_L$·H·A]$^+$, were monitored and isolated by broad-band ejection of the accompanying ions. The [**1**$_L$·H·A]$^+$ family was then allowed to react with the chiral amine B present in the cell at a fixed pressure whose value ranges from 8.7×10^{-8} to 4.7×10^{-7} mbar depending upon its reactivity.

The ESI-MS experiments with a Thermo Finnegan LCQ DECA XP Plus ion-trap mass spectrometer fitted with an electrospray ionization (ESI) source, equipped with a Model 75-72 nitrogen generator (Whatman Inc., Haverhill, MA, USA). Conditions are as follows: source voltage = +5.0 kV; sheath gas = 25 AU (arbitrary units); auxiliary gas = 10 AU; 8 capillary voltage = +3.3; capillary temperature = 180 °C; tube lens offset = +15 V. MS data were collected and processed using the Xcalibur Version 1.4 software.

3.3. NMR experiments

^{1}H and ^{13}C NMR spectra (300 and 75 MHz, respectively); TMS = 0 ppm as internal standard in $CDCl_3$. APT experiment was chosen to better distinguish between quaternary carbons, CH_2 carbons, and CD carbons (up) and CH carbons and CH_3 (down).

Acknowledgements

Work supported by the Ministero dell'Istruzione dell'Università e della Ricerca (MIUR, COFIN), the Consiglio Nazionale delle Ricerche (CNR) and Istituto Pasteur Fondazione Cenci Bolognetti. B.B. gratefully acknowledges Project "FIRB 2003" from MIUR (Ministero della Università e della Ricerca). The authors express their gratitude to F. Angelelli for technical assistance.

References

[1] B. Ganem, Y.T. Li, J.D. Henion, J. Am. Chem. Soc. 113 (1991) 6294.
[2] W. Mo, B.L. Karger, Curr. Opin. Chem. Biol. 6 (2002) 666.
[3] R. Aebersold, D.R. Goordlett, Chem. Rev. 101 (2001) 269.
[4] R. Aebersold, M. Mann, Nature 422 (2003) 198.

[5] J. Godovac-Zimmermann, L.R. Brown, Mass Spectrom. Rev. 20 (2001) 1.
[6] A. Pandey, M. Mann, Nature 405 (2000) 837.
[7] W.P. Blackstock, M.P. Weir, Trend Biotechnol. 17 (1999) 121.
[8] S. Dove, Nat. Biotechnol. 17 (1999) 233.
[9] J.A. Loo, Mass Spectrom. Rev. 16 (1997) 1.
[10] J.A. Loo, Int. J. Mass Spectrom. 200 (2000) 175.
[11] A.J. Heck, R.H.H. van den Heuvel, Mass Spectrom. Rev. 23 (2004) 368.
[12] B. Botta, M. Botta, A. Filippi, A. Tafi, G. Delle Monache, M. Speranza, J. Am. Chem. Soc. 124 (2002) 7658.
[13] A. Tafi, B. Botta, M. Botta, G. Delle Monache, A. Filippi, M. Speranza, Chem. Eur. J. 10 (2004) 4126.
[14] B. Botta, D. Subissati, A. Tafi, G. Delle Monache, A. Filippi, M. Speranza, Angew. Chem. Int. Ed. 43 (2004) 4767.
[15] B. Botta, F. Caporuscio, D. Subissati, A. Tafi, M. Botta, A. Filippi, M. Speranza, Angew. Chem. Int. Ed. 45 (2006) 2717.
[16] B. Botta, F. Caporuscio, I. D'Acquarica, G. Delle Monache, D. Subissati, A. Tafi, M. Botta, A. Filippi, M. Speranza, Chem. Eur. J. 12 (2006) 8096.
[17] A. Filippi, F. Gasparrini, M. Pierini, M. Speranza, C. Villani, J. Am. Chem. Soc. 127 (2005) 11912.
[18] A. Filippi, M. Speranza, Int. J. Mass Spectrom. 199 (2000) 211.
[19] As a matter of fact, the *slow* component of the bi-exponential kinetics of reaction (1) with A = **tyr**$^{\mathbf{OMe}}$ is due to its most stable [**1**$_{\mathbf{L}}$·H·**tyr**$^{\mathbf{OMe}}$]$^+$ regioisomer wherein the amino ester mainly protrudes from the chiral cavity of the host towards an external position between two adjacent pendants (ref. [16]).
[20] As suggested by one of the referees, the surprisingly high stability of the polar component corresponding to the complex between **1**$_{\mathbf{L}}$ and L-DOPA^{OEt} may be due to the formation of self-assembled **1**$_{\mathbf{L}}$/L-DOPA^{OEt} capsules composed of several resorcinarenes that surround several L-DOPA^{OEt} molecules (cfr. T. Evan-Salem, I. Baruch, L. Avram, Y. Cohen, L. C. Palmer, J. Rebek, Jr., Proc. Natl. Acad. Sci. USA 103 (2006) 12296). However, as reported in the text, no MS evidence is obtained in favour of the formation of such self-assembled **1**$_{\mathbf{L}}$/L-DOPA^{OEt} capsules.
[21] X. Cong, G. Czerwieniec, E. McJimpsey, S. Ahn, F.A. Troy, C.B. Lebrilla, J. Am. Soc. Mass Spectrom. 17 (2006) 442.
[22] S. Ahn, X. Cong, C.B. Lebrilla, S. Gronert, J. Am. Soc. Mass Spectrom. 16 (2005) 166.
[23] B. Botta, G. Delle Monache, P. Salvatore, F. Gasparrini, C. Villani, M. Botta, F. Corelli, A. Tafi, E. Gacs-Baitz, A. Santini, C.F. Carvalho, D. Misiti, J. Org. Chem. 62 (1997) 932.
[24] B. Botta, M.C. Di Giovanni, G. Delle Monache, M.C. De Rosa, E. Gacs-Baitz, M. Botta, F. Corelli, A. Tafi, A. Santini, E. Benedetti, C. Pedone, D. Misiti, J. Org. Chem. 59 (1994) 1532.
[25] T. Su, W.J. Chesnavitch, J. Chem. Phys. 76 (1982) 5183.